Nuclear levels of 228Th populated in the decay of 228Pa

W. Kurcewicz, K. Stryczniewicz, J. Zylicz, R. Broda, S. Chojnacki, W. Walus, I. Yutlandov

Classification
Physics Abstracts
12.10

NUCLEAR LEVELS OF ^{228}Th POPULATED IN THE DECAY OF ^{228}Pa

W. KURCEWICZ, K. STRYCZNIEWICZ J. ŻYLICZ

Institute of Nuclear Research, Dept of Physics IA, Świerk near Warsaw, Poland

R. BRODA (*), S. CHOJNACKI (**), W. WALUS (***) and I. YUTLANDOV

Joint Institute of Nuclear Research, Dubna, USSR

(*Reçu le 19 juin 1972, révisé le 13 octobre 1972*)

Résumé. — La désintégration ^{228}Pa $\rightarrow$ ^{228}Th a été amplement étudiée par des techniques diverses. Les spectres directs γ et X_K ont été mesurés avec des détecteurs Si(Li) et Ge(Li). Un ensemble de deux détecteurs Ge(Li) a été employé pour étudier les coïncidences γ-γ et γ-X_K. Un spectromètre magnétique toroïdal (avec fer) et un détecteur Ge(Li) ont été employés pour déterminer les coïncidences entre certaines raies de conversion interne et les transitions γ. Enfin les spectres des électrons de conversion ont été étudiés à l'aide d'un spectromètre β composé d'un détecteur Si(Li) et d'un système de diaphragmes placés dans un champ magnétique homogène. Le schéma des niveaux du ^{228}Th a été construit. Ce schéma, comprenant 39 niveaux, rend compte de 111 transitions parmi les 160, qui sont attribuées à la désintégration de ^{228}Pa. L'énergie de la désintégration par capture électronique a été déterminée égale à 2 103 $\left\{ \begin{smallmatrix} +16 \\ -12 \end{smallmatrix} \right.$ keV. Pour la capture électronique la distribution de l'intensité d'alimentation des niveaux de ^{228}Th est analysée en termes de modèles nucléaires. Certains aspects du mélange de Coriolis des quatre bandes octupolaires ($K = 0$, 1, 2 et 3) ont été étudiés. Les éléments de matrice de couplage, déduits de l'expérience, sont comparés aux résultats des calculs microscopiques.

Abstract, — The decay of ^{228}Pa to the levels of ^{228}Th has been extensively studied by various techniques. Single spectra of γ-and K X-rays have been measured with Si(Li) and Ge(Li) detectors. A set of two Ge(Li) detectors has been used to study γ-γ and γ-K X-ray coincidences. Measurements of γ-spectra in coincidence with the selected internal-conversion lines have been carried out using a Ge(Li) detector and a six-gap magnetic β-spectrometer. Finally, spectra of internal-conversion electrons have been studied in a β-spectrometer which uses a Si(Li) detector placed together with a system of diaphragms in a homogeneous magnetic field. The decay scheme has been constructed including 39 levels of ^{228}Th. It accounts for 111 of 160 transitions ascribed to the ^{228}Pa activity. The electron-capture decay energy has been determined to be 2 103 $\left\{ \begin{smallmatrix} +16 \\ -12 \end{smallmatrix} \right.$ keV. The strength distribution for the electron-capture feeding of the ^{228}Th levels is analysed in terms of nuclear models. The Coriolis mixing of four octupole bands ($K = 0$, 1, 2 and 3) is studied in some detail. The coupling matrix elements deduced from the experiment are compared with the results of the microscopic-model calculations.

1. **Introduction.** — Many features of the ^{228}Pa $\rightarrow$ ^{228}Th decay scheme were established and discussed by Arbman *et al.* [1] already in 1960. However, a decade later the available experimental techniques were much improved, mostly owing to the development of semiconductor detectors, and it seemed reasonable to reinvestigate this decay. The present paper describes such new extensive studies which led to a more complete knowledge of properties of the ^{228}Th levels. Among other results, the existence of $K = 0$, 2 and 3 octupole bands is confirmed and evidence is given tentatively for the previously unobserved $K = 1$ octupole band. The Coriolis coupling of these bands is analysed in some detail, reference being made to the microscopic-model calculations. Also the ^{228}Pa decay energy and branching ratios for the electron-capture feeding of the ^{228}Th levels are determined, which allows to calculate the distribution of the beta strength and to study this distribution in terms of nuclear models.

Permanent address :
(*) Institute of Nuclear Physics, Cracow, Poland.
(**) Institute of Experimental Physics, Warsaw University, Warsaw, Poland.
(***) Institute of Physics, Jagiellonian University, Cracow, Poland.

2. **Source preparations.** — The ^{228}Pa 22 h activity was produced in the ^{232}Th (p, 5 n) reaction. About 1 g of metallic thorium foil was bombarded for 3 to 6 h with 100 MeV protons in the JINR synchrocyclotron at Dubna. Protactinium samples were prepared by the chemical procedure briefly described by Kurcewicz *et al.* [2]. During the measurements, apart from the ^{228}Pa activity and traces of its decay products, contributions from ^{229}Pa, ^{230}Pa, ^{232}Pa and ^{233}Pa were observed.

3. **Singles spectra of γ-rays and internal-conversion electrons.** — The low-energy part of the γ-ray spectrum was measured with a 2.5 mm thick and 5 mm in diameter Si(Li) detector, having at 60 keV a resolution (FWHM) of 1.4 keV. The energy and intensity calibration was performed using the ^{57}Co, ^{109}Cd, ^{169}Yb and ^{241}Am sources.

The spectrum in the energy range of 100 to 2 100 keV was measured with several Ge(Li) detectors. The main results were obtained using a 5.6 cm^3 detector with a 1 600 channel analyzer and a 33 cm^3 detector with a 4 096 channel analyzer (Fig. 1 and 2). The resolution (FWHM) of these detectors at 1 332 keV was 3.0 and 4.0 keV, respectively. Energies of the intense γ-lines were determined from those of the standard lines by counting the ^{228}Pa source and standard sources simultaneously. In several runs, different sets of ^{22}Na, ^{60}Co, ^{88}Y, ^{110m}Ag, ^{207}Bi or ^{226}Ra standard sources were used. Also the energies of γ-lines of ^{230}Pa (Kurcewicz *et al.* [2]), ^{232}Pa (Kaczorowski *et al.* [3]) and ^{233}Pa were used as internal-calibration standards. The energies of ^{228}Pa lines with the assigned uncertainties of 0.2 keV or less were determined in this way. In the next step, these precisely determined energies were considered as secondary standards when finding the energies of weaker lines. For calibrating the efficiency of the detectors such sources as ^{56}Co, ^{110m}Ag and ^{226}Ra were used, which have several γ-lines with relative intensities accurately known. The intensity of some ^{228}Pa lines had to be corrected for the contribution from γ-lines of ^{230}Pa, ^{232}Pa or ^{233}Pa. Some of the γ-spectra were analysed using the GIER computer code.

The energy and intensity data for γ-rays of ^{228}Pa are listed in columns 1 and 2 of table I.

Column 3 of table I lists the data on relative intensities of the lines of internal-conversion electrons. A β-spectrometer with a 3 mm thick Si(Li) detector in a homogeneous magnetic field, described by Płochocki *et al.* [4], was used for detection of these lines in the energy range above 300 keV. Two parts of this spectrum are shown in figures 3 and 4. Since the detector was not thick enough to stop high-energy electrons completely, it was necessary to correct the line intensities for the detection efficiency. The efficiency curve was based on the data reported by Amov *et al.* [5] who studied the most intense ^{228}Pa conversion lines, in the energy range above 800 keV, using a high resolution magnetic β-spectrometer.

To calculate the internal-conversion coefficients, the γ-ray and conversion-line intensities were normalized

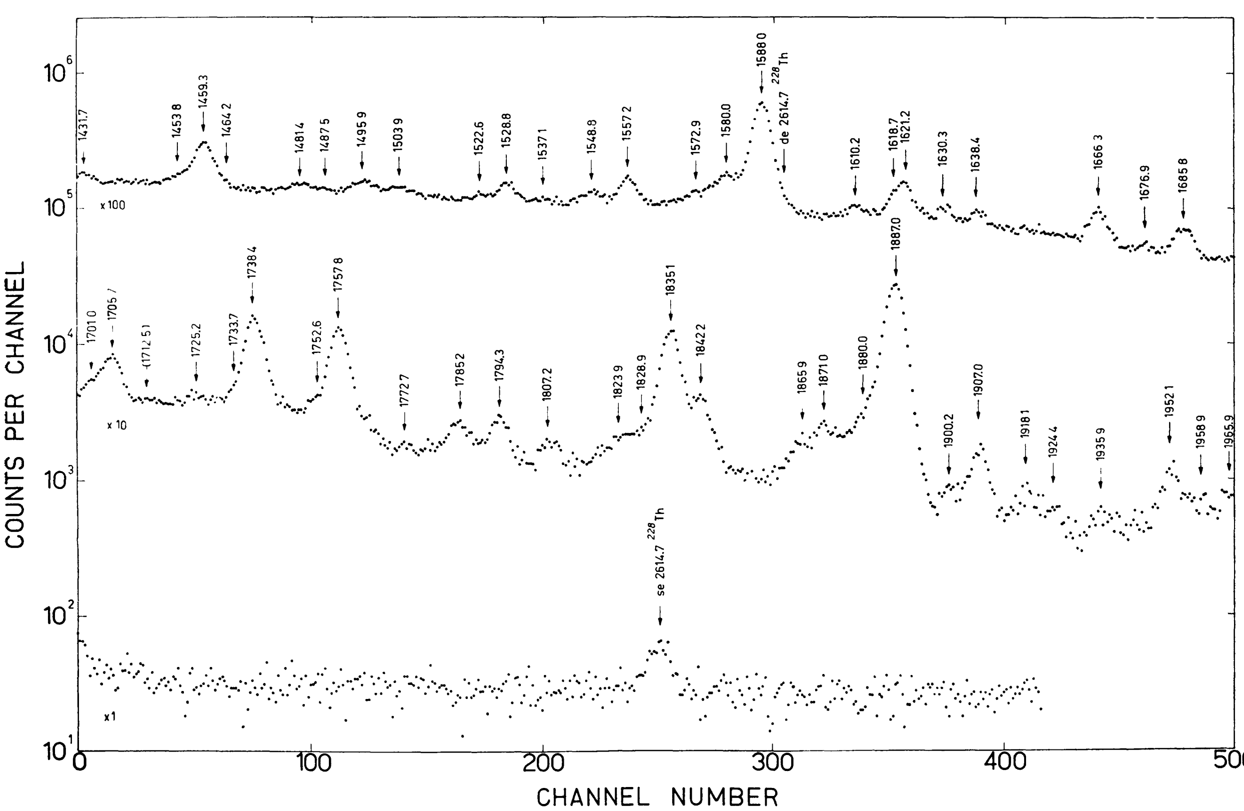

FIG. 1. — Singles γ-ray spectrum in the energy range above 1 400 keV taken using a 33 cm^3 Ge(Li) detector.

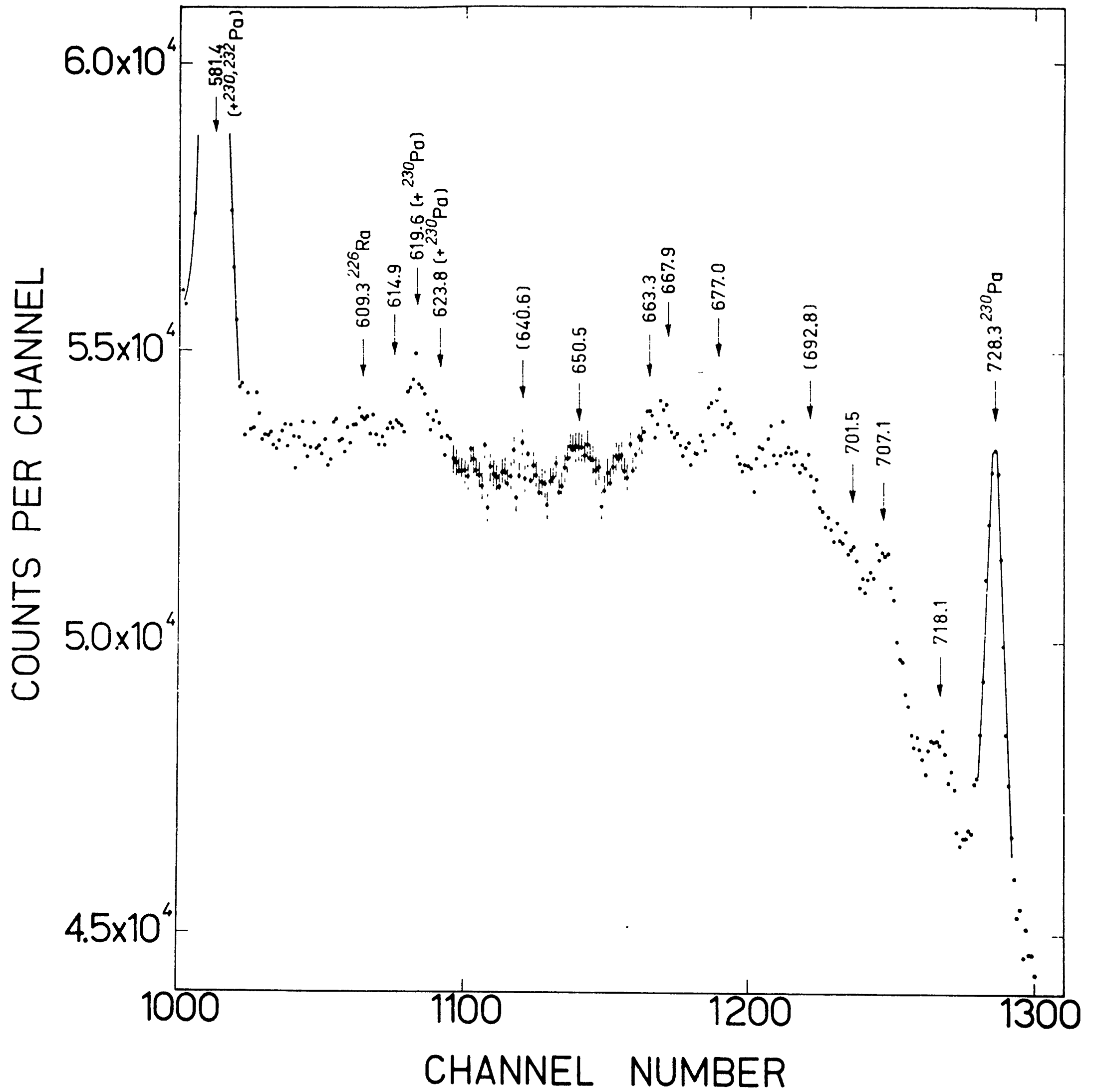

FIG. 2. — A section of the singles γ-ray spectrum showing several weak lines in the energy range from 600 keV to 720 keV.

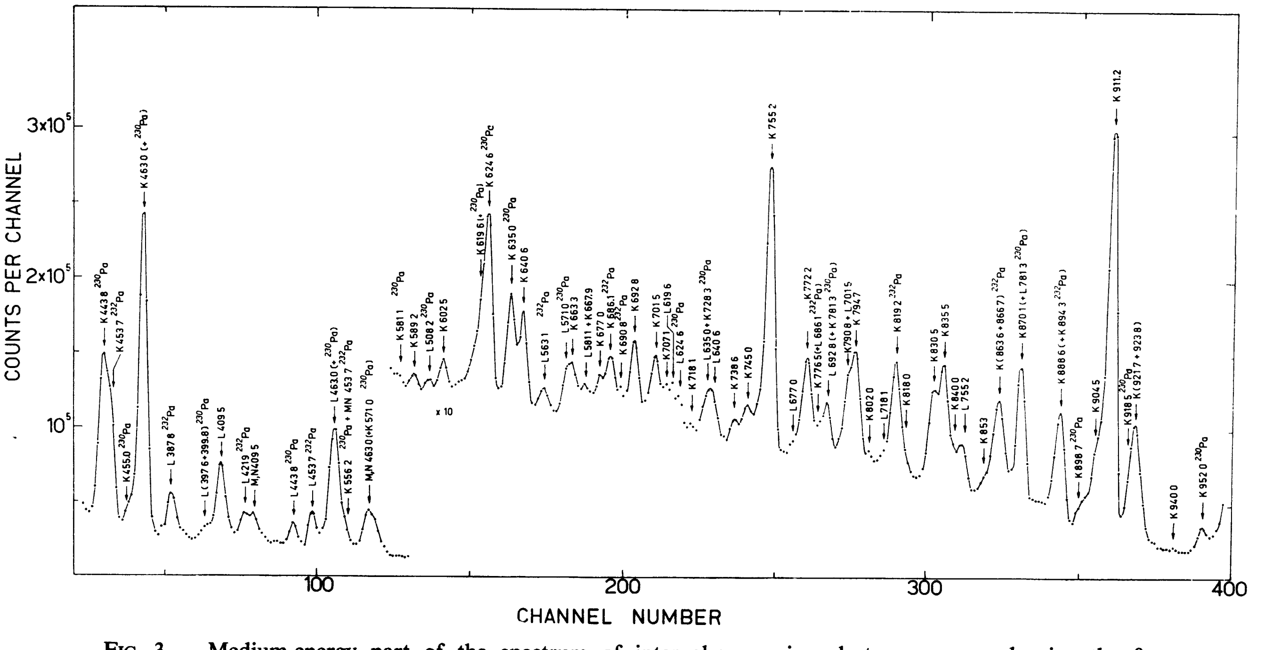

FIG. 3. — Medium-energy part of the spectrum of internal-conversion electrons measured using the β spectrometer with a Si(Li) detector in a homogeneous magnetic field.

TABLE I

Data on internal transitions in ^{228}Th

Energy (keV)	Intensity γ rays	Intensity K electrons	$\alpha_K \times 10^3$	Multipolarity	Initial level energy (e) (keV)
57.70 ± 0.10	87 ± 14			E 2 (a)	57.70
99.7 ± 0.3	36 ± 15			M 1 (a)	1 531.9
129.22 ± 0.10	475 ± 25			E 2 (a)	186.92
132.0 ± 0.6	77 ± 12				
138.3 ± 0.2	67 ± 10				
146.1 ± 0.3	54 ± 6				1 168.18
153.9 ± 0.3	60 ± 8				1 122.50
178.0 ± 0.2 (a)	⩽ 14	≈ 200 (a)	⩾ 3 400	M 1	1 200.4
184.5 ± 0.2 (a)	⩽ 30	520 ± 26 (a)	⩾ 4 100	E 0 + (M 1 + E 2)	1 153.6
191.2 ± 0.2	45 ± 7				378.1
199.7 ± 0.2	49 ± 6				1 168.18
204.4 ± 0.2	80 ± 7				1 226.56
209.28 ± 0.10	278 ± 25	88 ± 5 (a)	75 ± 9	E 1	396.09
210.0 ± 0.8 (b)	≈ 60 (b)				1 642.5
216.15 ± 0.10	145 ± 15				1 168.18
(219.8 ± 0.6)	≈ 30				1 944.5
223.61 ± 0.10	153 ± 13	780 ± 40 (a)	1 210 ± 120	M 1 + E 2	1 450.14
(240.2 ± 0.8) (b)	≈ 17 (b)				618.3
255 ± 1 (b)	≈ 50 (b)				1 687.3
270.23 ± 0.10	350 ± 17	48 ± 3 (a)	33 ± 3	E 1	327.74
278 (a)	⩽ 20	24 ± 1 (a)	⩾ 290	(M 1)	
281.87 ± 0.10	205 ± 11	512 ± 26 (a)	590 ± 45	M 1 + E 2	1 450.14
327.64 ± 0.10	660 ± 50	116 ± 6 (a)	42 ± 4	E 1 and E 2	327.74 and 1 450.14
332.36 ± 0.10	262 ± 24				519.28
338.32 ± 0.10	850 ± 50	68 ± 4 (a)	19 ± 2	E 1	396.06
341.1 ± 0.3	257 ± 20	56 ± 3 (a)	52 ± 5	E 2	1 432.00
409.51 ± 0.10	1 000 (f)	216 ± 11 (a)	51 ± 3	E 2	1 432.00
449.3 ± 0.6	≈ 50				1 900.00
(461 ± 1) (b)	≈ 140 (b)				1 892.6
463.00 ± 0.10	2 200 ± 100	394 ± 80	42 ± 9	E 2	1 432.00
481.3 ± 0.8	≈ 20				1 450.14
(498 ± 1) (b)	≈ 100 (b)				1 450.14
525.0 ± 0.6	30 ± 10				
547.5 ± 0.6	20 ± 5				
556.1 ± 0.5	30 ± 6				951.9
563.2 ± 0.5	110 ± 30				1 531.9
571.1 ± 0.2	95 ± 10				
573 ± 1 (b)	74 ± 20 (b)				969
581.4 ± 0.2	170 ± 40				1 645.7
589.2 ± 0.8	⩽ 13	1.6 ± 0.2	⩾ 26	M 1 + E 2	
602.5 ± 0.8	⩽ 10	3.2 ± 0.4	⩾ 66	M 1	
614.9 ± 0.4	16 ± 4				
619.6 ± 0.4	50 ± 20	9.8 ± 2.0	47 ± 21	M 1 + E 2	1 015.6
623.8 ± 0.5	13 ± 2				951.9 and/or 1 645.7
640.6 ± 0.5	10 ± 5	11 ± 2	260 ± 140	M 1	969
650.5 ± 0.4	42 ± 6				
663.3 ± 0.6	60 ± 8	6.4 ± 1.9	30 ± 10	M 1 + E 2	
667.9 + 0.6	65 ± 10	5.8 ± 1.7	21 ± 7	E 2	1 064.1
677.0 ± 0.4	97 ± 11	6.6 ± 1.3	16 ± 4	E 2	1 645.7
692.8 ± 0.8	9 ± 4	15.5 ± 2.3	410 ± 190	E 0 + (M 1 + E 2)	1 892.6
701.5 ± 0.5	13 ± 5	13.5 ± 2.0	250 ± 110	M 1	1 724.1
707.1 ± 0.2	50 ± 10	7.0 ± 2.0	33 ± 10	M 1 + E 2	1 226.56
718.1 ± 0.2	40 ± 2	2.1 ± 1.0	12 ± 6	(E 2)	1 687.3
726.2 ± 0.8 (b)	≈ 80 (b)				1 122.50
738.6 ± 0.6	⩽ 15	4.5 ± 1.0	⩾ 71	M 1	1 892.6 and/or 1 938.6
745.0 ± 0.6	⩽ 20	8.6 ± 1.3	⩾ 90	M 1	1 944.5
750.5 ± 0.5	35 ± 7				1 925.3
755.18 ± 0.10	210 ± 14	54.9 ± 2.8	62 ± 5	M 1	1 724.1
772.17 ± 0.10	198 ± 11	17.6 ± 1.4	21 ± 2	E 2 + M 1	1 168.18
776.5 ± 0.2	70 ± 8	3.0 ± 1.0	10 ± 3	E 2	
(782.0 ± 0.6) (b)	≈ 100 (b)				969.05
790.8 ± 0.3	45 ± 5	9.1 ± 1.8	48 ± 11	M 1	1 944.5

TABLE I (*continued*)

Energy (keV)	Intensity γ rays	Intensity K electrons	$\alpha_K \times 10^3$	Multipolarity	Initial level energy [e] (keV)
794.7 ± 0.2	334 ± 15	21.3 ± 3.4	15 ± 3	E 2 + M 1	1 122.50
(796 ± 1) [b]	≈ 20 [b]				1 174.7
802.0 ± 0.5	⩽ 15	2.8 ± 0.7	⩾ 44	M 1	
818.0 ± 0.8	100 ± 50	3.7 ± 1.1	8.8 ± 5.1	E 2	
823.5 ± 1.0	≈ 40				
830.5 ± 0.3	325 ± 16	18.0 ± 1.8	13 ± 2	E 2	1 226.56
835.5 ± 0.3	454 ± 23	22.7 ± 2.3	12 ± 2	E 2	1 022.36
840.0 ± 0.4	170 ± 10	6.5 ± 1.6	9.1 ± 2.4	E 2	1 168.18
853 ± 1	⩽ 10	2.0 ± 0.9	⩾ 47	M 1	1 944.5
870.1 ± 0.4	176 ± 10	26.8 ± 2.7	36 ± 4	M 1	1 892.6
884.2 ± 0.5	57 ± 12				1 900.0
888.6 ± 0.5	130 ± 30	2.9 ± 0.9	5.3 ± 2.0	E 1	
894.3 ± 0.5	440 ± 150				951.9
904.5 ± 0.3	480 ± 40	14.4 ± 2.2	7.1 ± 1.3	E 2	1 091.4
911.23 ± 0.10	2 670 ± 110	100	8.9 [d]	E 2	969.05
921.7 ± 0.3 [c]	⩽ 100	24.1 ± 3.2 [c]	⩾ 50	M 1	1 944.5
923.8 ± 0.5 [c]	≈ 60 [b]	10.8 ± 3.1 [c]	≈ 43	M 1	1 892.6
940.0 ± 0.8	100 ± 50	1.0 ± 0.2	2.3 ± 1.2	E 1	1 892.6
945.6 ± 0.8	300 ± 100				
957.8 ± 0.8	≈ 100				1 015.6
964.6 ± 0.3	1 680 ± 200	68 ± 27	9.6 ± 4.0	E 2	1 022.36
969.11 ± 0.10	2 200 ± 400	50 ± 20	5.4 ± 2.5	E 2	969.05 and 1 938.6
975.0 ± 0.3	260 ± 15	15 ± 3	14 ± 3	E 2 + M 1	1 944.5
987.8 ± 0.2	40 ± 2				1 174.7 and 2 010.0
1 018.6 ± 0.3	35 ± 5				
1 033.2 ± 0.3	80 ± 5				1 091.4
1 039.9 ± 0.3	28 ± 4				1 226.56
1 046.1 ± 0.8	6 ± 2				
1 054.4 ± 0.5	23 ± 6				1 450.14
1 065.2 ± 0.5	13 ± 1				1 122.50
1 070.2 ± 0.5	19 ± 4				
1 096.0 ± 0.8	5 ± 2				1 153.6
1 103.9 ± 0.8	3 ± 1				
1 110.4 ± 0.2	72 ± 3	0.55 ± 0.11	1.8 ± 0.4	E 1	1 168.18
1 118.6 ± 0.6	7 ± 1				
1 164.4 ± 0.6	12 ± 1	0.70 ± 0.07	14 ± 2	E 2 + M 1	
1 184.4 ± 0.6	4 ± 2	0.22 ± 0.06	13 ± 7	E 2, M 1	1 580.3
1 194.7 ± 1.0	3 ± 1	0.15 ± 0.05	12 ± 6	E 2, M 1	
1 237.7 ± 0.6	14 ± 2				
1 246.4 ± 0.2	150 ± 7	2.9 ± 0.3 [c]	4.6 ± 0.5	E 2	1 642.5
1 253.1 ± 0.6	3 ± 1	0.29 ± 0.08 [c]	23 ± 10	M 1	1 580.3
1 273.0 ± 0.6	13 ± 2				
1 288.0 ± 0.4	20 ± 1	0.72 ± 0.07	8.5 ± 1.0	E 2 + M 1	
1 298.0 ± 0.4	19 ± 2	0.21 ± 0.07	2.6 ± 0.9	E 1 + M 2	
1 311.0 ± 0.6	9 ± 3	0.26 ± 0.06	6.9 ± 2.7	E 2 + M 1	
1 420.6 ± 0.6	16 ± 1	0.34 ± 0.08	5.1 ± 1.2	E 2	
1 431.7 ± 0.6	23 ± 2	0.51 ± 0.09	5.3 ± 1.1	E 2	
1 453.8 ± 0.6	20 ± 1	0.13 ± 0.06	1.5 ± 0.7	E 1	
1 459.3 ± 0.2	120 ± 5	1.73 ± 0.30 [c]	3.4 ± 0.6	E 2	1 645.7
1 464.2 ± 0.2	10 ± 5				
1 481.4 ± 0.6	15 ± 1	0.30 ± 0.10	4.7 ± 1.6	E 2	
1 487.5 ± 0.6	≈ 9				
1 495.9 ± 0.4	28 ± 2	0.35 ± 0.10	3.0 ± 1.0	E 1, E 2	
1 503.9 ± 0.6	16 ± 1	0.16 ± 0.07	2.4 ± 1.1	E 1	1 900.0
1 522.6 ± 0.6	8 ± 1				1 580.3
1 528.8 ± 0.4	29 ± 2	0.40 ± 0.12	3.3 ± 1.1	E 1, E 2	1 925.3
1 537.1 ± 0.8	2 ± 1	0.26 ± 0.07	2.9 ± 1.5	E 2	1 724.1
1 548.8 ± 0.6	16 ± 1				1 944.5
1 557.2 ± 0.3	46 ± 2	1.1 ± 0.2	5.7 ± 1.2	E 2 + M 1	
1 572.9 ± 0.6	28 ± 5	0.34 ± 0.11	2.8 ± 1.0	E 1, E 2	1 900.0
1 580.0 ± 0.4	63 ± 6	0.45 ± 0.14	1.7 ± 0.5	E 1	1 580.3
1 588.0 ± 0.2	405 ± 18	4.1 ± 0.6 [c]	2.4 ± 0.4	(E 2)	1 645.7
1 610.2 ± 0.4	12 ± 1	0.58 ± 0.13	11 ± 3	M 1	
1 618.7 ± 0.4	23 ± 3	0.46 ± 0.15	4.7 ± 1.6	E 2 + M 1	1 676.3
1 621.2 ± 0.4	43 ± 4	1.3 ± 0.3	7.2 ± 1.7	M 1	

TABLE I (*continued*)

Energy (keV)	Intensity γ rays	Intensity K electrons	$\alpha_K \times 10^3$	Multipolarity	Initial level energy (^{e}) (keV)
—	—	—	—	—	—
1 630.3 $\pm$ 0.4	17 $\pm$ 2				1 687.3
1 638.4 $\pm$ 0.4	16 $\pm$ 2	0.23 $\pm$ 0.07	3.4 $\pm$ 1.1	E 2	2 016.4
1 666.3 $\pm$ 0.2	31 $\pm$ 2	1.2 $\pm$ 0.3 (^{c})	9.2 $\pm$ 2.4	M 1	1 724.1
1 676.9 $\pm$ 0.6	5 $\pm$ 1				1 676.3
1 685.8 $\pm$ 0.4	24 $\pm$ 2	0.33 $\pm$ 0.12	3.2 $\pm$ 1.2	E 2	
1 701.0 $\pm$ 0.6	10 $\pm$ 1				
1 705.7 $\pm$ 0.4	36 $\pm$ 2	0.9 $\pm$ 0.2	5.9 $\pm$ 1.3	E 2 + M 1	1 892.6
(1 712.5 $\pm$ 0.6)	$\approx$ 2				1 900.0
1 725.2 $\pm$ 0.6	4 $\pm$ 1				
1 733.7 $\pm$ 0.8	7 $\pm$ 2				
1 738.4 $\pm$ 0.2	106 $\pm$ 5	2.60 $\pm$ 0.26 (^{c})	5.8 $\pm$ 0.7	E 2 + M 1	1 925.3
1 752.6 $\pm$ 0.6	5 $\pm$ 1				1 938.6
1 757.8 $\pm$ 0.2	90 $\pm$ 5	1.50 $\pm$ 0.30 (^{c})	3.9 $\pm$ 0.8	E 2 + M 1	1 944.5
1 772.7 $\pm$ 0.6	5 $\pm$ 1				
1 785.2 $\pm$ 0.3	14 $\pm$ 1	0.28 $\pm$ 0.14	4.7 $\pm$ 2.4	E 2 + M 1	1 842.9
1 794.3 $\pm$ 0.3	15 $\pm$ 1				
1 807.2 $\pm$ 0.5	5.4 $\pm$ 0.4	0.16 $\pm$ 0.08	7.0 $\pm$ 3.6	E 2 + M 1	1 993.9
1 823.9 $\pm$ 0.8	6 $\pm$ 1				2 010.0
1 828.9 $\pm$ 0.8	9 $\pm$ 2				2 016.4
1 835.1 $\pm$ 0.2	106 $\pm$ 6	1.56 $\pm$ 0.23 (^{c})	3.5 $\pm$ 0.6	E 2 + M 1	1 892.6
1 842.2 $\pm$ 0.3	27 $\pm$ 2	0.60 $\pm$ 0.20 (^{c})	5.2 $\pm$ 1.8	E 2 + M 1	1 900.0 and/or 1 842.9
1 865.9 $\pm$ 0.6	8 $\pm$ 1				
1 871.0 $\pm$ 0.6	15 $\pm$ 2	0.18 $\pm$ 0.09	2.8 $\pm$ 1.4	(E 2)	
1 880.0 + 0.8	23 $\pm$ 2				1 938.6
1 887.0 $\pm$ 0.2	260 $\pm$ 15	2.97 $\pm$ 0.45 (^{c})	2.7 $\pm$ 0.4	E 2	1 944.5
1 900.2 $\pm$ 0.6	2.6 $\pm$ 0.3				1 900.0
1 907.0 $\pm$ 0.4	9.8 $\pm$ 0.5				1 965.0
1 918.1 $\pm$ 0.6	2.8 $\pm$ 0.3				
1 924.4 $\pm$ 0.6	1.4 $\pm$ 0.3				
1 935.9 $\pm$ 0.6	2.4 $\pm$ 0.3				1 993.9
1 952.1 $\pm$ 0.6	8.5 $\pm$ 0.6				2 010.0
1 958.9 $\pm$ 0.8	3.6 $\pm$ 0.5				2 016.4
1 965.9 $\pm$ 0.8	4.8 $\pm$ 0.6				1 965.0

(^{a}) Data from reference [1] ; K-electron intensities are renormalized by the present authors and assumed to be accurate within about 5 % (see caption to table I in ref. [1]).
(^{b}) Data from our coincidence measurements.
(^{c}) Data from reference [5].
(^{d}) Based on assumption of E 2 multipolarity for the 911.23 keV transition.
(^{e}) For the transitions placed in the decay scheme, see Fig. 10*a* and 10*b*.
(^{f}) The intensity of 1 000 units corresponds to 7.4 % of the ^{228}Pa decay rate.

by assuming the theoretical (Hager and Seltzer [6]) E 2 internal-conversion coefficient of 8.9×10^{-3} for the 911.23 keV transition. The columns 4 and 5 in table I list, respectively, the values of the internal-conversion coefficients and the multipolarity assignments, deduced by comparing these values with the theoretical ones [6].

4. **Coincidence measurements.** — The γ-spectra in coincidence with internal-conversion electrons were measured using a 5.6 cm^3 Ge(Li) detector and a six-gap magnetic β-spectrometer. The conditions of these measurements were identical to those in ^{230}Pa studies of Kurcewicz *et al.* [2]. The results are presented in figures 5 and 6, and in table II.

TABLE II

Results of the eγ coincidence studies

Selected conversion line	Energies (keV) and intensities (in brackets) of coincident γ lines
—	—
L 57.7	209 (250 $\pm$ 50), 270 (254 $\pm$ 57), 282 (160 $\pm$ 60), 332 (290 $\pm$ 70), 338 (890 $\pm$ 100), 410 (950 $\pm$ 110), 463 (1 330 $\pm$ 150), 498 ? ($\approx$ 100), 830 ($\approx$ 250), 835 and/or 840 ($\approx$ 390), 894 ? ($\approx$ 150), 905 ($\approx$ 420), 911 ($\equiv$ 2 670), 965 (1 780 $\pm$ 330)
L 129.3	191 (41 $\pm$ 15), 209 (264 $\pm$ 23), 224 (39 $\pm$ 12), 240 ? ($\approx$ 17), 255 (32 $\pm$ 11), 282 (42 $\pm$ 14), 332 (240 $\pm$ 25), 341 (205 $\pm$ 24), 410 (360 $\pm$ 41), 707 (105 $\pm$ 47), 772 ? ($\approx$ 110), 782 ? ($\approx$ 105), 796 ? ($\approx$ 20), 830 (180 $\pm$ 85), 835 ($\equiv$ 450), 870 ($\approx$ 50), 905 (390 $\pm$ 65), 988 ? ($\approx$ 90)

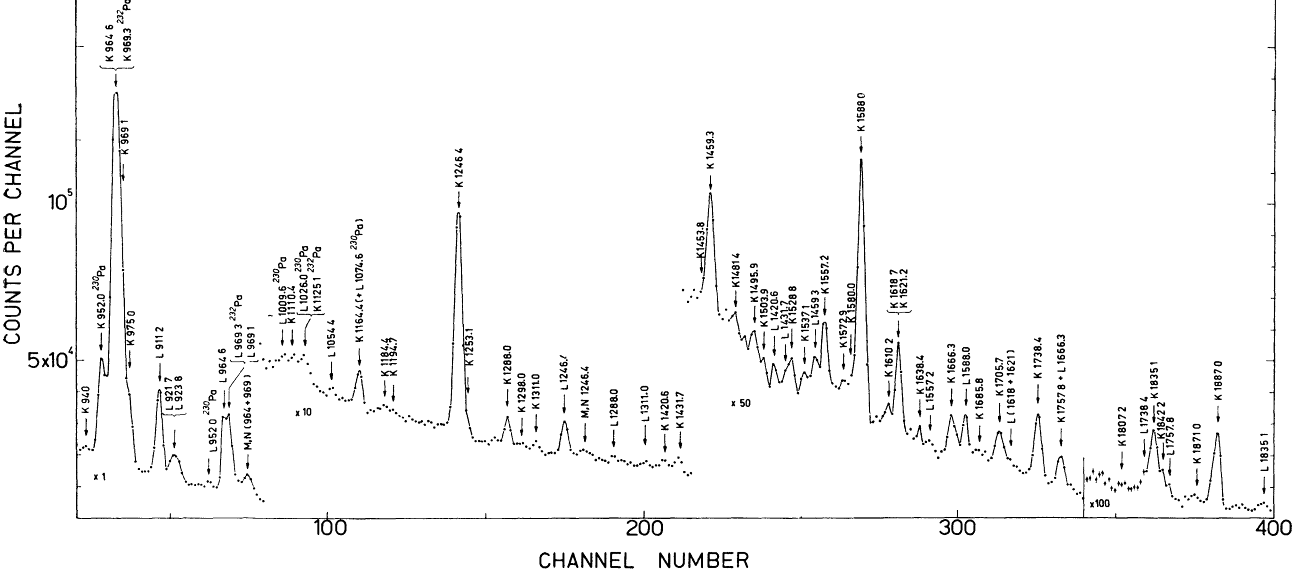

FIG. 4. — High-energy part of the spectrum of internal-conversion electrons measured using the β spectrometer with a Si(Li) detector in a homogeneous magnetic field.

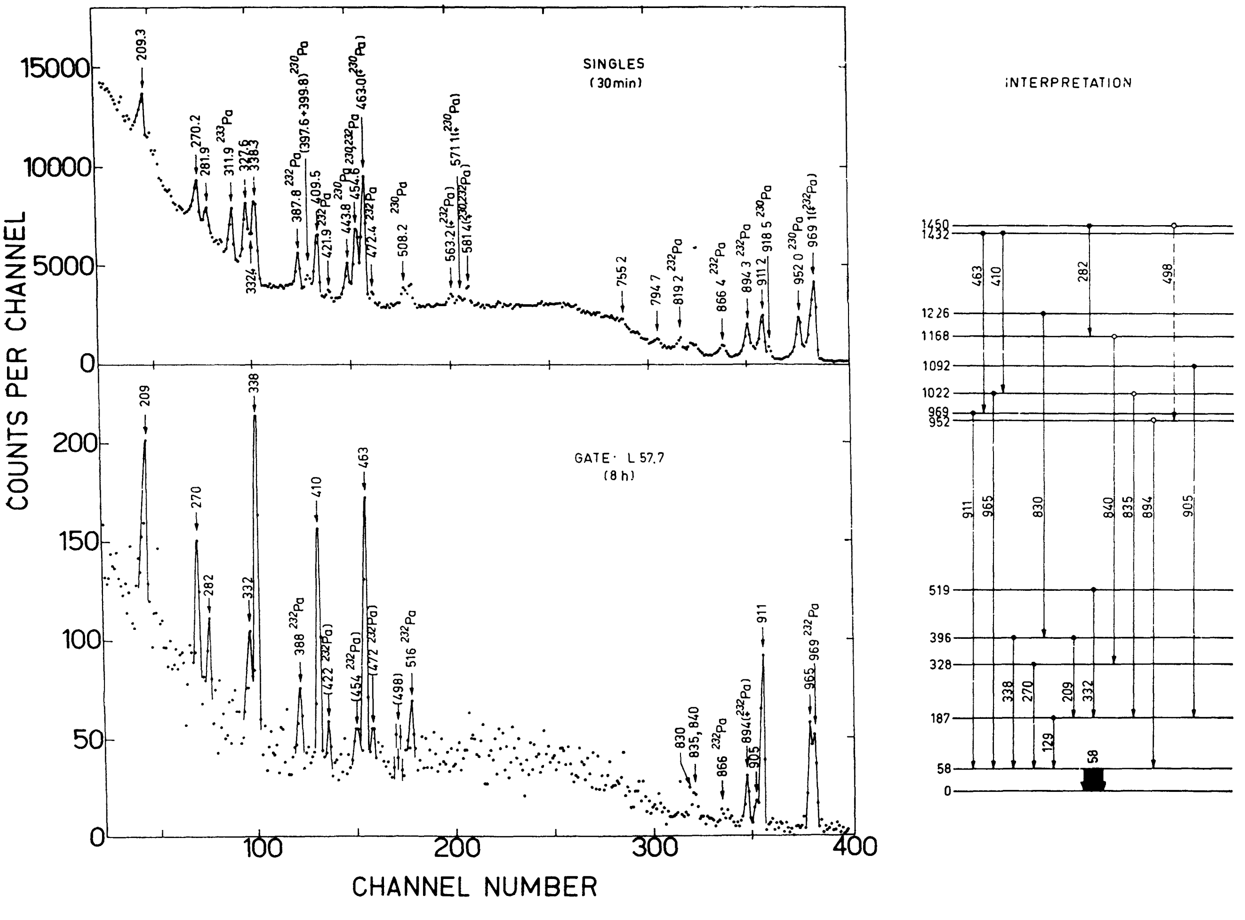

FIG. 5. — Gamma-ray spectrum coincident with the L 57.7 internal-conversion line and its interpretation.

The measurements of γ-γ coincidences were performed using a spectrometer with two Ge(Li) detectors. These detectors were placed at an angle of about 60° with regard to the source position. Absorbers were used to stop γ-rays scattered from one detector in the direction of the other one. A fast-slow coincidence circuit with a time-to-amplitude converter was applied. Two coincidence spectra were recorded simultaneously. One was gated by a selected γ-line and a portion of the Compton continuum, and the second one by a

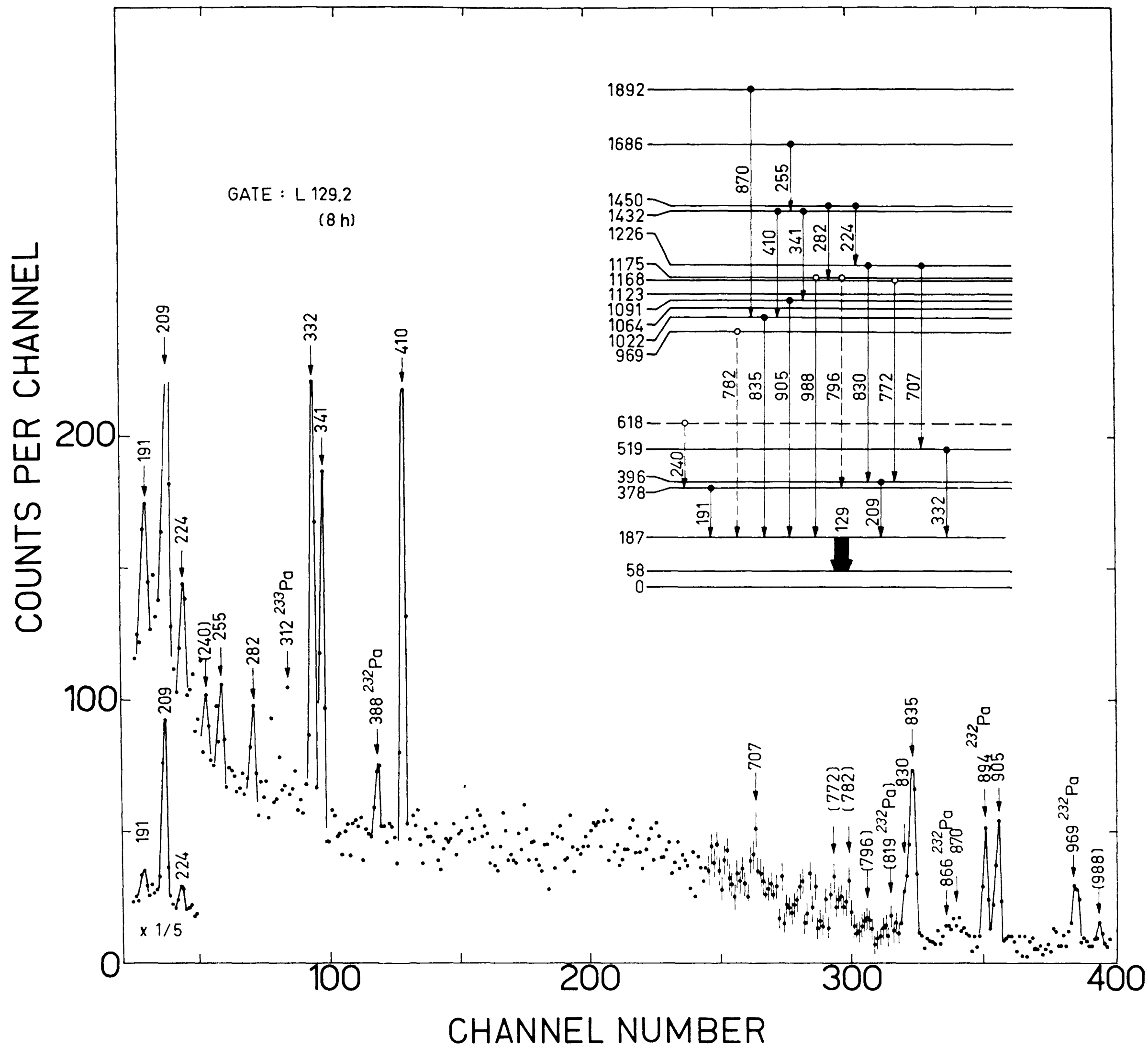

FIG. 6. — Gamma-ray spectrum coincident with the L 129.2 internal-conversion line and its interpretation.

section of this continuum above the line. Thus the pure coincidence effect due to the selected transition could be deduced. In figure 7 a typical pair of coincidence spectra is shown by way of example. As it may be seen from table III, the coincidence data were obtained for five gating lines.

TABLE III

Results of the $\gamma\gamma$ coincidence studies

Selected energy interval (keV)	γ lines (keV)	Energies (keV) and intensities (in brackets) of coincident γ lines
260-280	270	282 (71 $\pm$ 27), 328 (312 $\pm$ 62), 795 ($\equiv$ 334), 840 (153 $\pm$ 44)
330-350	338	224 (40 $\pm$ 8), 282 (35 $\pm$ 12), 328 (26 $\pm$ 13), 480 (36 $\pm$ 17), 556 ? ($\approx$ 50), 573 (74 $\pm$ 20), 619 (31 $\pm$ 16), 668 ? ($\approx$ 50), 726 (51 $\pm$ 20), 772 ($\equiv$ 198), 830 (250 $\pm$ 40), 870 (24 $\pm$ 14), 1 246 (100 $\pm$ 36)
	341	905 ($\equiv$ 480), 1 033 (120 $\pm$ 50)
400-420	410	129 (174 $\pm$ 34), 210 (65 $\pm$ 20), 461 ? (145 $\pm$ 50), 520 (60 $\pm$ 36), 835 (470 $\pm$ 95), 965 ($\equiv$ 1 680)
790-810	795	270 ($\equiv$ 350), 328 (820 $\pm$ 250)
900-920	905	341 (124 $\pm$ 30).
	912	154 (53 $\pm$ 21), 328 (47 $\pm$ 25), 463 ($\equiv$ 2 200), 481 ? ($\approx$ 60), 707 ($\approx$ 20), 755 (290 $\pm$ 70), 923 ($\approx$ 60), 975 (180 $\pm$ 60)

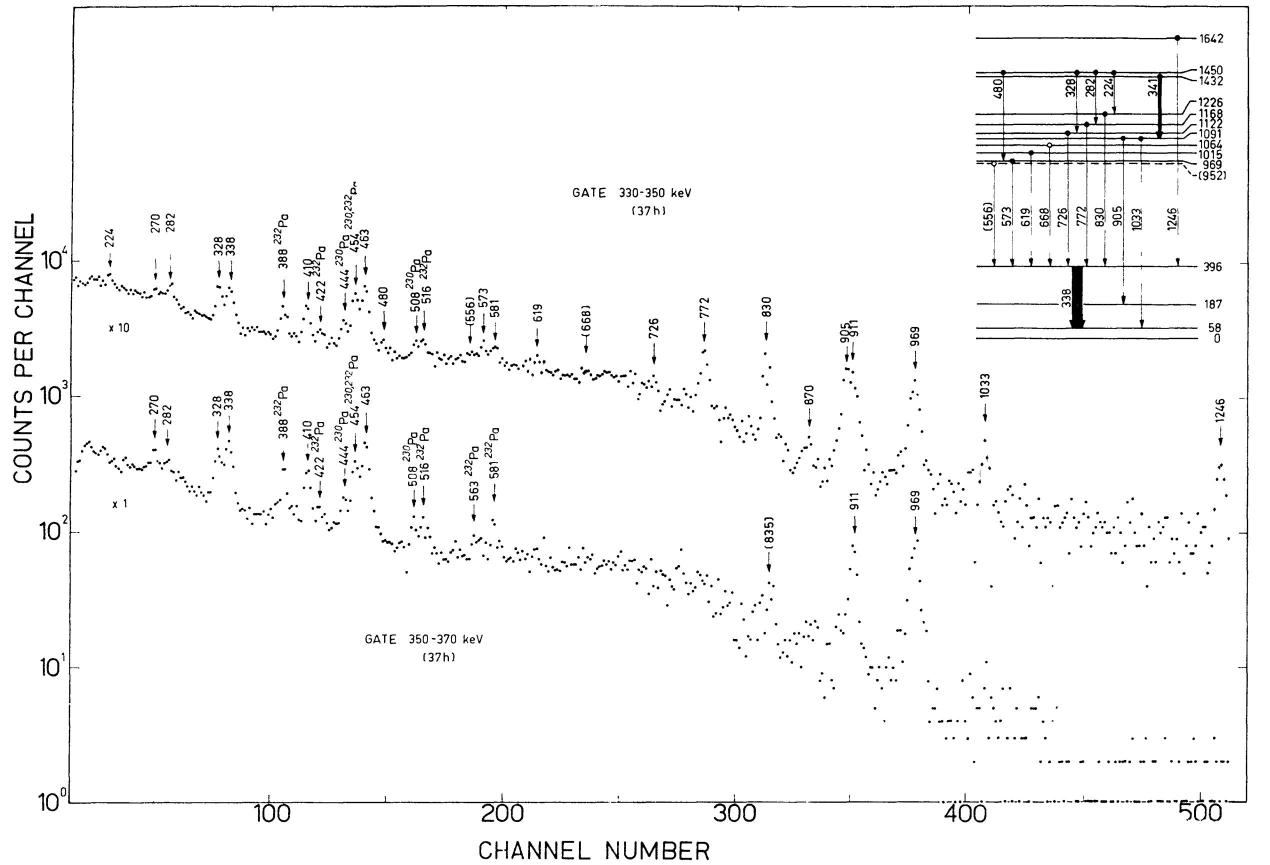

FIG. 7. — Gamma-ray spectrum measured in coincidence with the 338.3 keV γ-line and its interpretation. The spectrum coincident with the fraction of the Compton distribution is shown or comparison. The gating transition was taken using a 4.5 cm³ Ge(Li) detector, and the coincident spectrum-using a 13 cm³ Ge(Li) detector.

5. **Determination of the electron-capture decay energy.** — The method used to determine the ^{228}Pa decay energy Q_{EC} was similar to that described by Kurcewicz *et al.* [2] for the decay of ^{230}Pa. It takes account of the well known dependence of the relative K-capture probability P_K upon the electron-capture transition energy Q.

The ratio of the intensities was determined experimentally for the 1 588 and 1 887 keV γ-lines from the singles γ-ray spectrum and the spectrum coincident with the K X-rays (cf. Fig. 8). From these data it was possible to calculate the ratio of the P_K values for the electron-capture transitions to the levels at 1 646 and 1 945 keV (cf. Fig. 9). This ratio was found to be 0.47 $\pm$ 0.11, where from the energy for the transition to the 1 945 keV level is equal to 158 $\left\{ \begin{matrix} +16 \\ -12 \end{matrix} \right.$ keV. Thus, the decay energy is $Q_{EC} = 2\,103 \left\{ \begin{matrix} +16 \\ -12 \end{matrix} \right.$ keV.

6. **The decay scheme.** — The ^{228}Pa decay scheme shown in figures 10*a* and 10*b* is an extension of that published by Arbman *et al.* [1]. The twenty one levels of ^{228}Th reported in reference [1] have been confirmed, and new levels at 618, 952, 969 (2⁻), 1 016, 1 064, 1 175, 1 200, 1 580, 1 642, 1 676, 1 843, 1 900, 1 925, 1 939, 1 965, 1 994, 2 010 and 2 016 keV have been

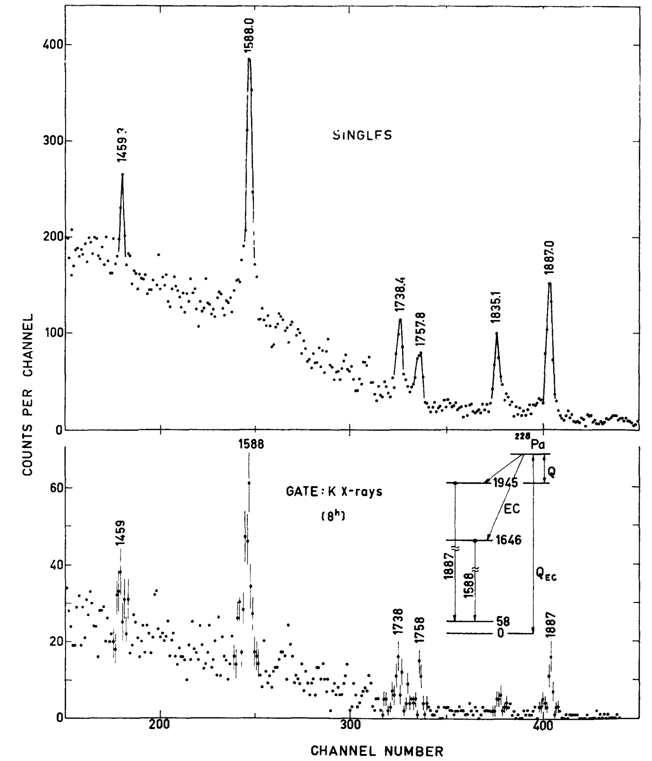

FIG. 8. — Section of the singles γ-ray spectrum and of the spectrum coincident with K X-rays. In the insert a fragment of the decay scheme is shown.

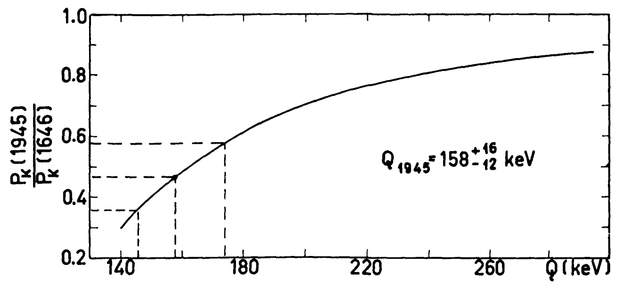

FIG. 9. — Dependence of the P_K (1 945)/P_K (1 646) ratio as a function of the energy Q of the EC transition to the 1 945 keV level. The experimental value of this ratio, obtained in the coincidence measurements (see Fig. 8), is also presented.

found. It has recently been shown that many of these new levels are populated also in the β^--decay of ^{228}Ac (Dalmasso and Maria [7], Herment and Vieu [8], Herment [9]).

The construction of the ^{228}Th level scheme is based on the transition energy fits, searched with the use of a special computer program, and on the results of the coincidence experiments. The decay scheme includes 111 of the total number of 160 transitions ascribed to the ^{228}Pa activity. The multipole character established for numerous transitions allows to define the parity for the majority of the ^{228}Th levels and to assign spin values to many of them. With the knowledge

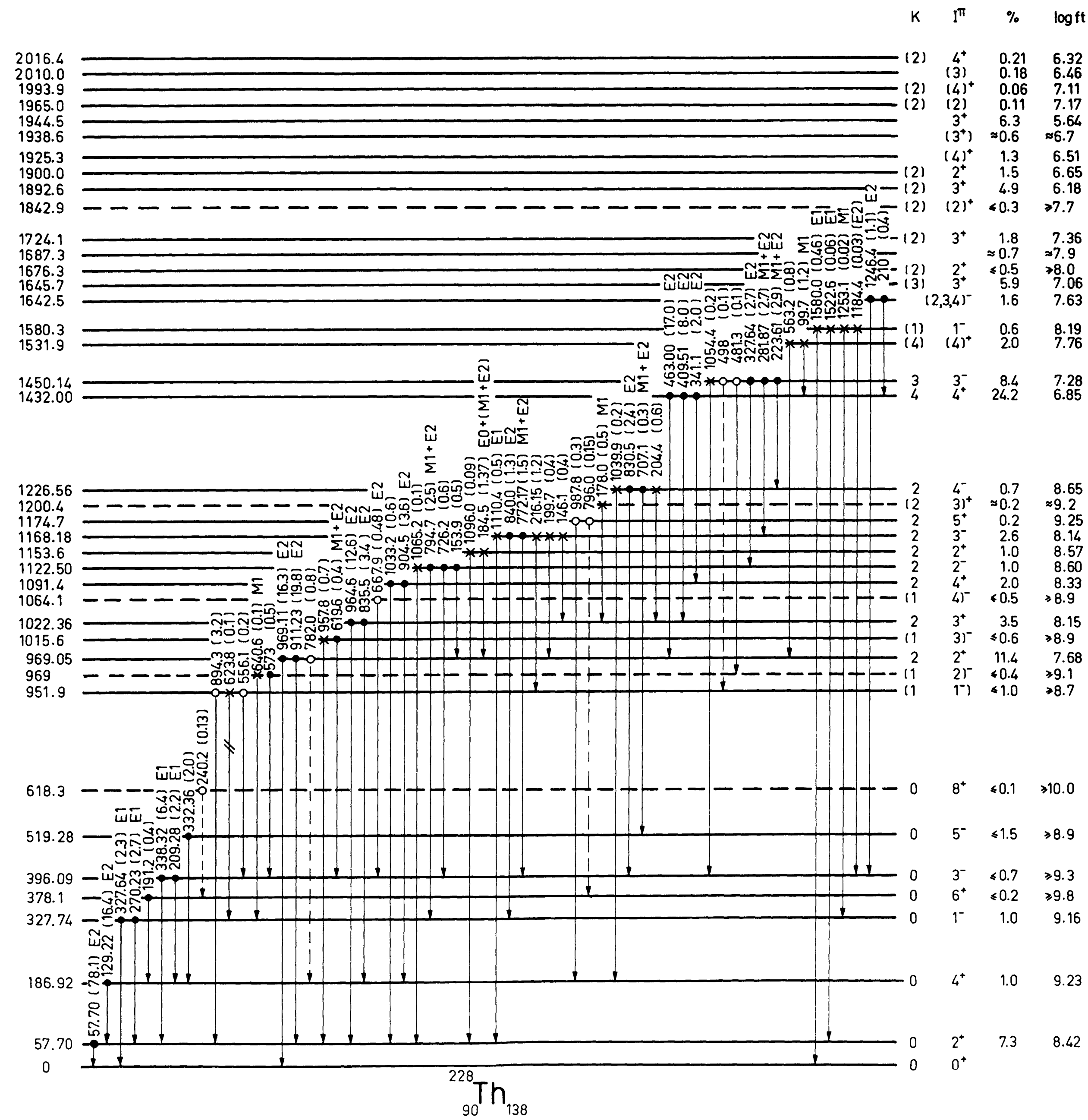

FIG. 10*a*. — Scheme of the ^{228}Pa decay to ^{228}Th levels. The spacing of close-lying levels is not up to scale. The internal transitions, whose position in the decay scheme has been established or suggested by coincidence measurements, are marked with full and open circles, respectively. Crosses refer to the transitions placed on the basis of the energy fit alone. Transitions placed in two alternative positions are marked with two bars. The intensities (in parentheses) of the transitions are given in per cent of the ^{228}Pa decays. All energies are in keV.

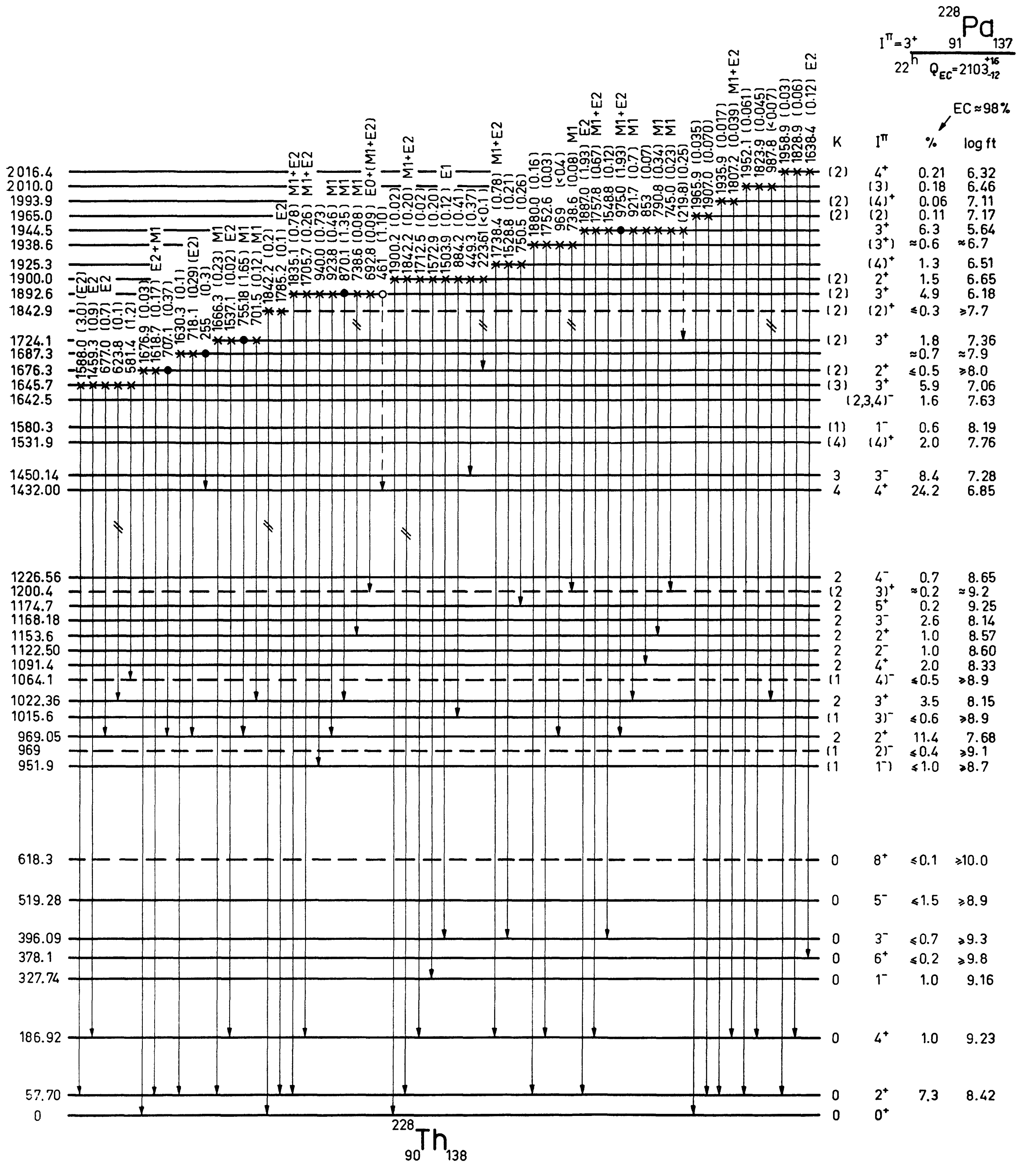

FIG. 10*b*. — Scheme of the ²²⁸Pa decay to ²²⁸Th levels (for comments cf. caption to Fig. 10*a*).

of the Q_{EC} value, of the ^{228}Pa half-life and of the EC branching ratios it was possible to calculate log *ft* values. The low log *ft* value for the transition to the 1 944 keV 3^+ level and the direct EC feeding of the 2^+ and 4^+ levels indicates the spin and parity 3^+ for the ^{228}Pa ground state. This is in agreement with the assignment proposed by Arbman *et al.* [1]. The assignments of the K quantum numbers to the levels at lower excitation energy results from the interpretation of these levels in terms of nuclear models (cf. section 7).

The arguments taken into account when constructing the decay scheme can be easily reproduced if use is made of the information contained in tables I-III. It has been decided, therefore, to omit in this section any comments on the existence of individual levels in ^{228}Th and on the spin-parity assignment. In the next section, however, brief comments can be found on several, mostly tentative, levels whose identification is important for the verification of the applicability of the deformed-nuclei theory to low-energy excitations in ^{228}Th.

The balance of the intensities for the decay scheme is based on the assumption that the EC process occurs in 98 % of the ^{228}Pa decays (see tables by Lederer *et al.* [10]) and that there is no EC feeding of the ^{228}Th ground state. The total transition intensities have been calculated with the use of the theoretical internal conversion coefficients of Hager and Seltzer [6]. The intensity of the 49 transitions not included in the decay scheme corresponds to that of about 11 % of the total EC decays. Including of these transitions in the decay scheme would result in a change of the EC branchings and log *ft* values with respect to those given in figures 10*a* and 10*b*. This, however, could hardly affect the spin and parity assignment to the ^{228}Pa ground state. We believe also that the qualitative conclusions of section 7.3 on the beta-strength distribution would not be changed.

7. **Discussion.** — The properties of the ^{228}Th levels are discussed in this section in terms of the models developed for the deformed nuclei. For a general presentation of these models the reader may refer to Nathan and Nilsson [11] and Soloviev [12].

7.1 POSITIVE-PARITY STATES BELOW 1 500 keV. — The interpretation of the low-energy ^{228}Th levels of positive parity is illustrated in figure 11.

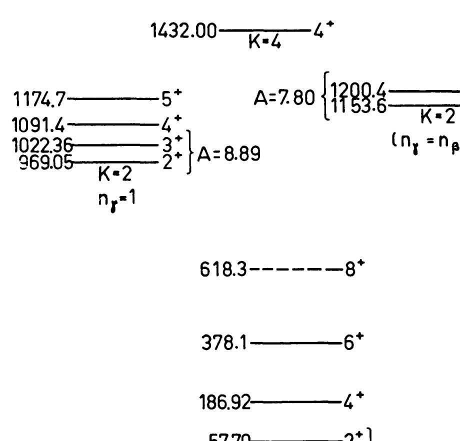

FIG. 11. — Interpretation of the ^{228}Th positive-parity states below 1 500 keV. Notation : A — moment-of-inertia parameter in keV, n_β and n_γ — quantum numbers of the β and γ oscillations, respectively.

The ground-state band is shown with four rotational levels. The 6^+ level introduced by Arbman *et al.* [1] as uncertain is now well proved by coincidence data. The evidence for the 8^+ level is only tentative. The calculations based on the rotational formula, with three parameters determined from the position of the 2^+, 4^+ and 6^+ levels, for the 8^+ level yield the energy of 624 keV. This is not far from the tentatively given experimental value.

The new level at 1 174.5 keV, also observed in the decay of ^{228}Ac (Herment [9]), is interpreted as the spin-parity 5^+ member of the γ-vibrational band. The β-vibrational 0^+ level, introduced by Lederer *et al.* [13] at 0.83 MeV, has not been found to be fed in the decay of ^{228}Pa.

The 1 153.6 keV level and the γ-vibrational bandhead state are linked by the E 0 transition (1). Hence, for the 1 153.6 keV level we have $KI^\pi = 22^+$, and therefore this level could be interpreted as a two-phonon $(\beta + \gamma)$-state. Its energy is, however, significantly lower than the sum of the energies of the β-and γ-vibrational levels. Similar $K^\pi = 2^+$ levels have been observed in ^{230}Th (see ref. [2] and earlier papers quoted there) and in ^{234}U (Bjørnholm *et al.* [15]).

The assignment of $KI^\pi = 44^+$ to the 1 432.0 keV level has been concluded from the ratios of the E 2 reduced probabilities of the transitions to the γ-band. The experimental ratios

$$\begin{gathered} B(E\,2,\ 44^+ \to 22^+) : B(E\,2,\ 44^+ \to 23^+) : \\ B(E\,2, 44^+ \to 24^+) = \\ (1.12 \pm 0.08) : 1 : (0.64 \pm 0.05) \end{gathered}$$

are in agreement with the theoretical ones, 1.04 : 1 : 0.61, obtained from the Mihailov formula [16] with the parameter $a = 0.030$. No agreement is achieved when $KI^\pi = 33^+$ is assumed for the decaying state. A possible two-quasiparticle configuration of this state is discussed in section 7.3.

7.2 OCTUPOLE BANDS. — The negative-parity states observed in ^{228}Th below 1 500 keV are interpreted as members of the octupole bands (cf. Fig. 12).

The existence of the $K = 0$, 2 and 3 octupole bands observed by Arbman *et al.* [1] has been confirmed in the present study. The reduced branching ratios for the transitions deexciting these bands are found to be consistent with the adopted interpretation, provided that the analysis is carried out with the use of the Mihailov formula [16].

A new octupole band with $K = 1$ is proposed to have its first four levels at 951.9, 969, 1 015.6 and 1 064.1 keV.

The 951.9 keV *level.* — To this level a spin and parity 1^- may be assigned only tentatively. The 1^- level may be expected to decay to the 0^+ ground state. The fact that such a transition has not been observed in the γ-ray spectrum does not necessarily contradict this assignment, since it can be masked by the strong

(1) The EO character of the 184.5 keV transition was earlier noticed by Bjørnholm [14]. Reference should also be made to the publication by Herment and Vieu [8].

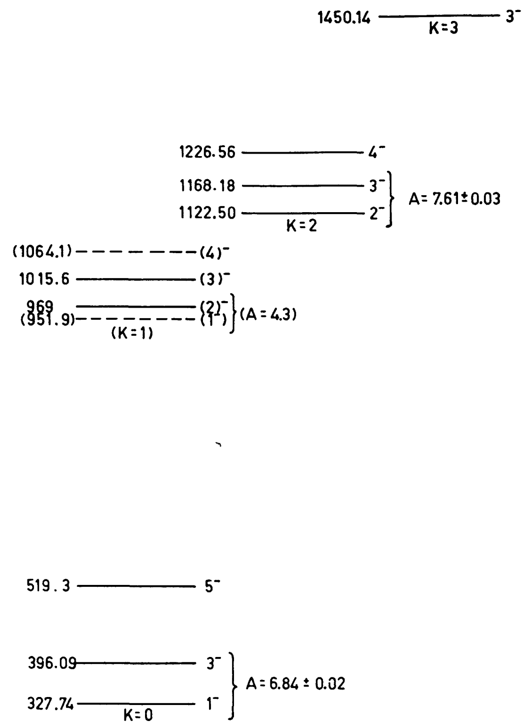

FIG. 12. — Octupole bands in ^{228}Th. A — moment-of-inertia parameter in keV.

951.92 keV line of ^{230}Pa. This level may be interpreted as the head of a new band.

The 969 keV *level.* — The $KI^{\pi} = 12^-$ level at 969 keV is proposed mainly because of its decay to the 396.09 keV $KI^{\pi} = 03^-$ and 327.74 keV $KI^{\pi} = 01^-$ levels. The 573 keV transition appears in coincidence with the 338.32 keV line. We believe that this is a M 1 or E 2 transition from the 969 keV 12^- level rather than a K-forbidden E 1 transition from the 969.05 keV 22^+ level. The 640.6 keV transition is placed between the hypothetical 2^- and the 327.74 keV 1^- levels for the energy-fit reason, without any coincidence support. However, its M 1 character is consistent with our interpretation.

The 1 015.6 keV *level.* — The existence of this level is well proved by coincidence data. Also it is shown clearly that its parity is negative. This level is a candidate to be interpreted as a 3^- member of the $K^{\pi} = 1^-$ band.

The 1 064.1 keV *level.* — This level could be the 4^- state of the $K^{\pi} = 1^-$ band, but its existence should be considered as tentative.

If the $K^{\pi} = 1^-$ band has the level energies as suggested here, it is for the first time possible, anyway to the present author's knowledge, to get some information on the Coriolis interaction of all four one-phonon octupole bands directly from experiment. In the calculations performed it has been necessary to consider several quantities as free parameters : (i) three coupling matrix elements A_{01}, A_{12} and A_{23} (the subscripts referring to the K values) and (ii) the unperturbed energy of the $KI^{\pi} = 33^-$ level. The moment-of-inertia parameter A has been assumed to be the same for all bands. For the sake of simplicity, the relations between A, A_{01} and A_{12}, derived from the known positions of the $I = 1$ and $I = 2$ levels in the $K = 1$ and 2 bands, have been used in the calculations, the small experimental errors being neglected. A fit of the calculated energies to the experimental ones has been performed for the four $I = 3$ levels. The values of the matrix elements found in this way are listed in table IV, and compared with the theoretical expectations.

TABLE IV

Matrix elements of the Coriolis interaction between octupole bands (in keV)

$A_{K,K+1}$	Experiment (^{a})	Theory (^{b})	(^{c})	(^{d})
A_{01}	31.5	32.0	42.3	7.2
A_{12}	21.5	29.2	41.9	44.1
A_{23}	35.5	22.6	—	60.4

(^{a}) From the analysis of the level-energy spacings. The inertial parameter A = 8.34 keV.

(^{b}) The spherical-limit values calculated according to the formula given by Neergård and Vogel [18].

(^{c}) Based on microscopic calculations by Zheleznova *et al.* [17].

(^{d}) Based on microscopic calculations by Błocki [19].

For the parameter values resulting from the best-fit procedure adopted here, the energies of the 1^- and 2^- levels are reproduced exactly and those of the 3^- levels — within $\pm$ 0.6 keV. The agreement between the calculated and experimental energies for the 4^- levels is worse. For the $K = 1$ and $K = 2$ bands, the calculated energies of the 4^- levels are 1 039.4 and 1 234.2 keV, respectively, which is pretty far from the experimental values.

The experimental energies of the levels of the ^{228}Th octupole bands are compared in table V with the theoretical results based on the microscopic-model calculations carried out by different authors.

7.3 DISTRIBUTION OF THE BETA STRENGTH IN THE ^{228}Pa $\rightarrow$ ^{228}Th DECAY. — In the considerations of the ^{228}Pa EC decay given below, the most probable configuration of the Nilsson-model orbitals, p 530 ↑ and n 752 ↑, has been assumed for the ground state of this nucleus, in agreement with Arbman *et al.* [1].

The rather low probability (low strength) observed for the $\Delta K = 3$ EC decay to the levels of the ground-state band and of the $K^{\pi} = 0^-$ octupole band of ^{228}Th is related to the effect of K forbiddenness. Also, the $\Delta K = 2$ value for the 1st forbidden transitions to the levels of the possible $K^{\pi} = 1^-$ octupole band eliminates all matrix elements, except the unique

TABLE V

Energy levels of octupole bands in ^{228}Th

K	I^π	Experiment this work	Energy (keV) Ref. [17]	Ref. [20]	Ref. [18]	Ref. [21]
0	1^-	328	350	620	360	460
	3^-	396			400	
	5^-	519				
1	1^-	952	1 110	1 020	880	1 100
	2^-	969			890	
	3^-	1 016			980	
	4^-	1 064				
2	2^-	1 122	1 600	1 160	1 130	1 400
	3^-	1 168			1 200	
	4^-	1 227				
3	3^-	1 450		1 530	1 420	

one, which is compatible with the high limits set for log ft values as given in the decay scheme.

The allowed transitions to the gamma-vibrational band, as well as the 1st-forbidden non-unique transitions to the $K^\pi = 2^-$ and 3^- octupole bands, are not hindered by the K selection rule. To explain the low rate of transitions to the first two of these bands qualitatively, we may refer to the microscopic-model calculations performed by Zheleznova *et al.* [17]. They show for both collective wave functions a very low contribution of those two-quasiparticle configurations which can presumably participate in the EC transformation. The transition to the $KI^\pi = 33^-$ state at 1 450 keV is faster (log ft = 7.28). This fact seems to be in a strong disagreement with the results of calculations performed by Błocki [19] who has found that the 3^- state in question has an almost pure (98.5 %) two-proton configuration (541 ↓ + 642 ↑), which cannot be fed in the EC decay of ^{228}Pa. Zheleznova *et al.* [17] do not give any explicit information on the structure of the 3^- states.

Table VI contains a list of those pure two-quasiparticle states, predicted by the superconductivity model, which have proper configurations from the point of view of their direct EC feeding from the ^{228}Pa ground state, and which are theoretically predicted at energies below 2.4 MeV.

The transitions occurring in this case are either allowed hindered or 1 st-forbidden unhindered, for which we assume log ft values of 6.5 and 7.0, respectively. It should be realized that the experimental information about the beta transitions between the quasiparticle states of odd-A actinide nuclei is very scarce and, therefore, our estimate of the log ft values contains a large uncertainty.

The (752 ↑ + 761 ↑) configuration may possibly be ascribed to the 4^+ level observed at 1 432 keV. However, identification of other two-quasiparticle states,

TABLE VI

Two-quasiparticle levels in ^{228}Th *fed by allowed and first forbidden* EC *decay of* ^{228}Pa

Two-quasiparticle states Configuration	Energy (MeV)	Spin and parity	log ft (assumed)
nn (752 ↑ + 631 ↑)	1.31	4^-	7.0
nn (752 ↑ + 761 ↑)	1.44	4^+	6.5
nn (752 ↑ ± 770 ↑)	1.71	$2^+, 3^+$	6.5
nn (752 ↑ ± 640 ↑)	1.76	$2^-, 3^-$	7.0
nn (752 ↑ ± 501 ↓)	1.97	$2^+, 3^+$	6.5
nn (752 ↑ ± 631 ↓)	2.11	$2^-, 3^-$	7.0
pp (530 ↑ + 651 ↑)	1.12	2^-	7.0
pp (530 ↑ + 532 ↓)	1.36	2^+	6.5
pp (530 ↑ + 642 ↑)	1.40	3^-	7.0
pp (530 ↑ + 523 ↓)	1.41	3^+	6.5
pp (530 ↑ + 521 ↑)	2.00	2^+	6.5
pp (530 ↑ + 633 ↑)	2.10	4^-	7.0

Energies calculated by Błocki and Kurcewicz (unpublished). The version of the superconductivity model used in these calculations has been earlier described in reference [19] and [20].

at higher energy, would be difficult not only because of the lack of complete experimental information on spins, parities, log ft values or deexcitation patterns, but also due to the expected level-mixing effects. It has been decided, therefore, to analyse the distribution of the average beta strength rather than probabilities of individual transitions. The energy range of the ^{228}Th excitations defined by the value of Q_{EC} has been divided into $\Delta E = 0.3$ MeV intervals and for each interval the beta strength

$$S = \frac{1}{\Delta E} \sum \frac{1}{ft}$$

has been calculated. The results are shown in figure 13. Except for one energy interval, the experimental beta-strength distribution is lower than the analogous distribution calculated on the basis of the table VI data. Some excess of the strength observed between 1.8 and 2.1 MeV could be perhaps an indication of the role of the four-quasiparticle configuration n 752 ↑, n 631 ↑, p 530 ↑, p 631 ↓. Such a state would be fed by a fast, allowed unhindered transition. Admixtures of this four-quasiparticle configuration to some of the even-parity states in the considered energy interval can explain the appearance of the enhancement of the beta decay to these states.

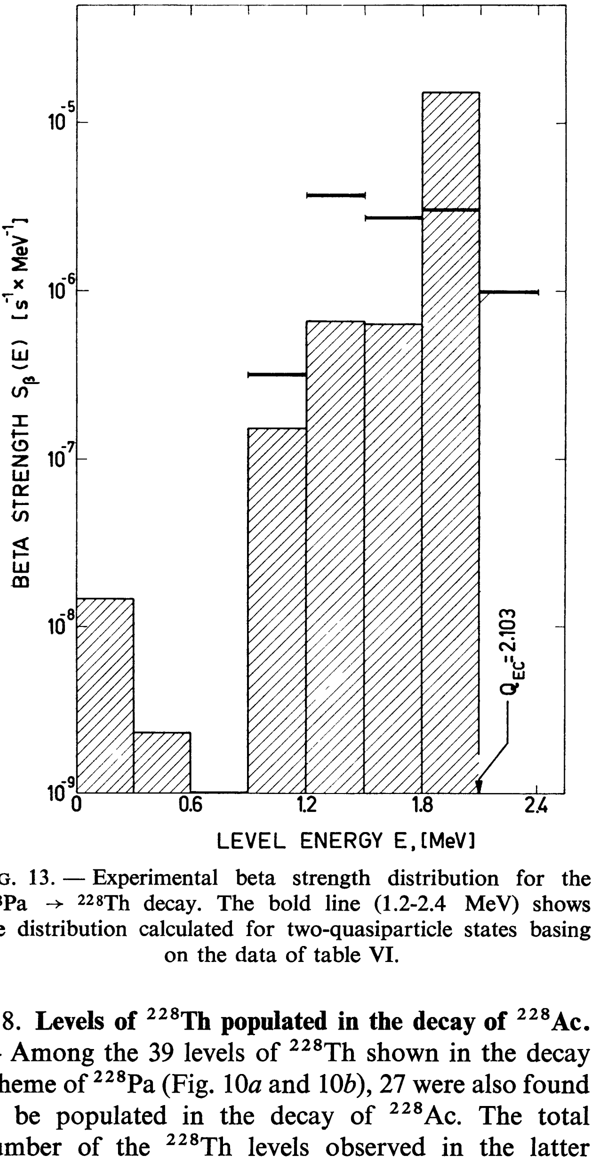

FIG. 13. — Experimental beta strength distribution for the ^{228}Pa → ^{228}Th decay. The bold line (1.2-2.4 MeV) shows the distribution calculated for two-quasiparticle states basing on the data of table VI.

8. **Levels of ^{228}Th populated in the decay of ^{228}Ac.** — Among the 39 levels of ^{228}Th shown in the decay scheme of ^{228}Pa (Fig. 10*a* and 10*b*), 27 were also found to be populated in the decay of ^{228}Ac. The total number of the ^{228}Th levels observed in the latter decay is 49 (Dalmasso and Maria [7], Herment and Vieu [8], Herment [9]). The few differences in the results obtained both from studies of the ^{228}Pa and ^{228}Ac decays, which are of importance from the point of view of the discussion developed in sections 7.1 and 7.2, are briefly commented below.

The 969 keV *level.* — In the ^{228}Ac → ^{228}Th decay scheme, Herment [9] (see also ref. [7] and [8]) shows only one level at 969 keV and interprets it as the γ-vibrational state. There is no suggestion as to the existence of the negative-parity level at approximately the same energy. However, its existence may now be considered as certain, since the arguments given in section 7.2 (e. g. the M 1 character of the 640 keV transition) are now strengthened by the fact that Herment places the 640 keV transition between the 969 keV and 328 keV 3^- levels not only basing on the energy fit but also on coincidence studies.

The 1 016 keV *level.* — From the M 1 + E 2 character of the 620 keV transition, placed on the basis of the coincidence experiment between the 1 016 keV and 396 keV 3^- levels, the present authors deduce the negative parity for the 1 016 keV state (section 7.2). On the other hand Herment, who places the 620 keV transition in the same way but having no evidence for its character, suggests that the 1 154 keV $(2)^+$ and 1 026 keV levels may be connected by the 138 keV (M 1 + E 2) transition. This would indicate the positive parity of the 1 016 keV state. Since there is no coincidence evidence for such a placing of the 138 keV transition, the assignment of the negative parity to the 1 016 keV level seems more probable.

The 1 432 keV *level.* — The existence of the 308 keV (presumably E 1) transition between the 1 432 keV and 1 123 keV 2^- levels, as shown in the ^{228}Ac → ^{228}Th decay scheme by Herment, would mean that the present authors would have to abandon the $KI^\pi = 4{,}4^+$ assignment proposed in section 7.1 for the 1 432 keV state. The spin value could not be higher than 3, which is actually the assignment suggested by Herment. On the other hand it is difficult to learn from reference [9] how good is the evidence for the existence and placing of the 308 keV transition. This transition has not been observed in the present study of the ^{228}Pa decay (the upper limit for the intensity of the 308 keV γ-line is 30 units in the scale adopted for table I). Thus, the problem of the spin of the 1 432 keV level seems to remain open.

A part of the present study was performed at the Joint Institute for Nuclear Research in Dubna, and the authors wish to thank professor Flerov and his co-workers for their hospitality. They are also grateful to Drs. J. Błocki and J. Jastrzębski, Institute of Nuclear Research in Świerk, for valuable discussion of the results.

References

[1] ARBMAN E., BJØRNHOLM S. and NIELSEN O. B., *Nucl. Phys.*, **21** (1960), 406.

[2] KURCEWICZ W., STRYCZNIEWICZ K., ŻYLICZ J., CHOJNACKI S., MOREK T. and YUTLANDOV I., *Acta Phys. Polon.*, **B 2** (1971), 451.

[3] KACZOROWSKI R., KURCEWICZ W., PŁOCHOCKI A. and ŻYLICZ J., *Acta Phys. Polon.*, **B 2** (1971), 423.

[4] PŁOCHOCKI A., BELCARZ E., SŁAPA M., SZYMCZAK M. and ŻYLICZ J., *Nucl. Instr. and Meth.*, **92** (1971), 85.

[5] Amov B. G., Kotlińska B. and Kurcewicz W., *Acta Phys. Polon.*, **B 2** (1971), 337.
[6] Hager R. S. and Seltzer E. C., *Nuclear Data*, **4** (1968), 1.
[7] Dalmasso J. and Maria H., *C. R. Acad. Sci., Paris*, **B 273** (1971), 568.
[8] Herment M. and Vieu Ch., *C. R. Acad. Sci., Paris*, **B 273** (1971), 1058.
[9] Herment M., Thèse, Faculté des Sciences de l'Université de Grenoble, 1971.
[10] Lederer C. M., Hollander J. M. and Perlman I., Table of Isotopes, John Wiley, N. Y., 1967.
[11] Nathan O. and Nilsson S. G., Chapitre X in « Alpha-, Beta- and Gamma-Ray Spectroscopy » edited by K. Siegbahn, North-Holland Publishing Company, Amsterdam, 1965.
[12] Soloviev V. G., Theory of Complex Nuclei, « Nauka », Moscow, 1971.
[13] Lederer C. M., Thesis, Report UCRL-11028, 1963.
[14] Bjørnholm S., private communication.
[15] Bjørnholm S., Borgreen J., Davis D., Hansen N. J. S., Pedersen J. and Nielsen H. L., *Nucl. Phys.*, **A 118** (1968), 261.
[16] Mihailov V. M., *Izv. Akad. Nauk SSSR, Ser. Fiz.*, **30** (1966), 1334.
[17] Zheleznova K. M., Kornejtchuk A. A., Soloviev V. G., Vogel P. and Jungklaussen G., JINR Report D-2157, Dubna, 1965.
[18] Neergård K. and Vogel P., *Nucl. Phys.*, **A 149** (1970), 209.
[19] Błocki J., Thesis, Institute of Nuclear Research, Report 1292/IA/PL, Warsaw, 1971.
[20] Błocki J. and Kurcewicz W., *Phys. Lett.*, **30 B** (1969), 458.
[21] Komov A. L., Malov L. A. and Soloviev V. G., JINR Report P 4-5126, Dubna 1970.